doi:10.26443/seismica.v5i1.1902

Did they blow it? Time-lapse velocity variations during an open-pit mine slope failure using seismic noise interferometry

Tjaart de Wit * [1,2], **Roelof Snieder** [1]

[1]Center for Wave Phenomena, Dept. of Geophysics, Colorado School of Mines, Golden, CO, USA, [2]Applied Geophysics Department, Institute of Mine Seismology, Kingston, Tasmania, Australia

Author contributions: *Conceptualization*: T. de Wit. *Software*: T. de Wit. *Formal Analysis*: T. de Wit. *Writing - Original draft*: T. de Wit. *Writing - Review & Editing*: R. Snieder, T. de Wit. *Visualization*: T. de Wit. *Supervision*: R. Snieder.

Abstract Landslides are geological events that directly impact thousands of people every year and cause significant loss of life. Landslides are often triggered by extreme weather events or earthquakes. While most slope monitoring approaches focus on surface deformation (e.g. using radar), in some cases by the time changes manifest at surface, it can be too late to provide adequate early warning. Seismic ambient noise correlation has been successfully applied in landslide monitoring, but has yet to be applied on the slope of an open-pit mine. This approach measures time-lapse seismic velocity changes in the subsurface of a slope. Several cases of precursory changes have been shown using seismic ambient noise correlation and shows promise in providing early warning of failure. We present a case study from a dense borehole geophone array installed beneath a well-instrumented slope of an open-pit mine in Australia. We applied seismic ambient noise correlation across a period of slope failure and measured a decrease in seismic velocity approximately 12 days prior to the initiation of the slope failure. We investigated this change and its relationship to seismicity, rainfall and surface deformation recorded during this period.

Production Editor:
Andrea Llenos
Handling Editor:
Christos Evangelidis
Copy & Layout Editor:
Hannah F. Mark

Received:
August 6, 2025
Accepted:
February 20, 2026
Published:
March 1, 2026

Non-technical summary Landslides are geological events that directly impact thousands of people every year and cause significant loss of life. While many slope monitoring approaches focus on surface displacements, in many cases by the time changes manifest at the surface, it can be too late to provide adequate early warning. This paper investigates a slope failure at an open-pit mine in Australia using a technique called seismic interferometry. This method analyses background vibrations in the ground (seismic noise) to detect changes in the subsurface. About 12 days before the slope failed, we detected a decrease in seismic velocity beneath the slope, likely indicating weakening from fracturing within the slope. The study demonstrates that seismic interferometry can detect changes beneath the surface before a slope failure occurs to potentially provide an early warning system for an impending mining accident, saving lives and reducing economic losses.

1 Introduction

Landslides are a geological hazard that directly impact thousands of people around the world every year, and have the potential to cause huge economic damage (Sim et al., 2022) and significant loss of life (Petley, 2012; Froude and Petley, 2018). Landslides are often triggered by extreme weather events (most notably heavy rainfall) or shaking from earthquakes (Wieczorek, 1996; Sim et al., 2022). Human activities such as construction, excavation for roads, and illegal mining, have been shown to play an increasing role in the growing incidence rate of landslides (Froude and Petley, 2018). With the impacts of climate change expected to accelerate the melting of permafrost in mountainous areas and increase the occurrence of extreme weather events, landslides are anticipated to pose a greater threat in the future particularly in already vulnerable regions around the world (Gariano and Guzzetti, 2016).

As a result, the assessment and on-going monitoring of known landslides plays an essential role in risk mitigation and disaster prevention. Modern landslide monitoring techniques generally focus on continuous monitoring of slope displacements. These techniques include ground based monitoring using technology such as inclimometers, extensometers, Global Navigation Satellite System (GNSS) stations, or Real Aperture Radar (RAR), and various remote sensing techniques such as Interferometry Synthetic Aperture Radar (InSAR). These techniques each have their own set of challenges and limitations (Carlà et al., 2019; Lissak et al., 2020). Some ground based techniques, for example, are limited to just a few ground points and remote sensing techniques like InSAR provide infrequent measurements due to low satellite revisit rates or seasonal snow cover in high alpine regions of interest, impacting their reliability.

*Corresponding author: tjaartdewit@mines.edu

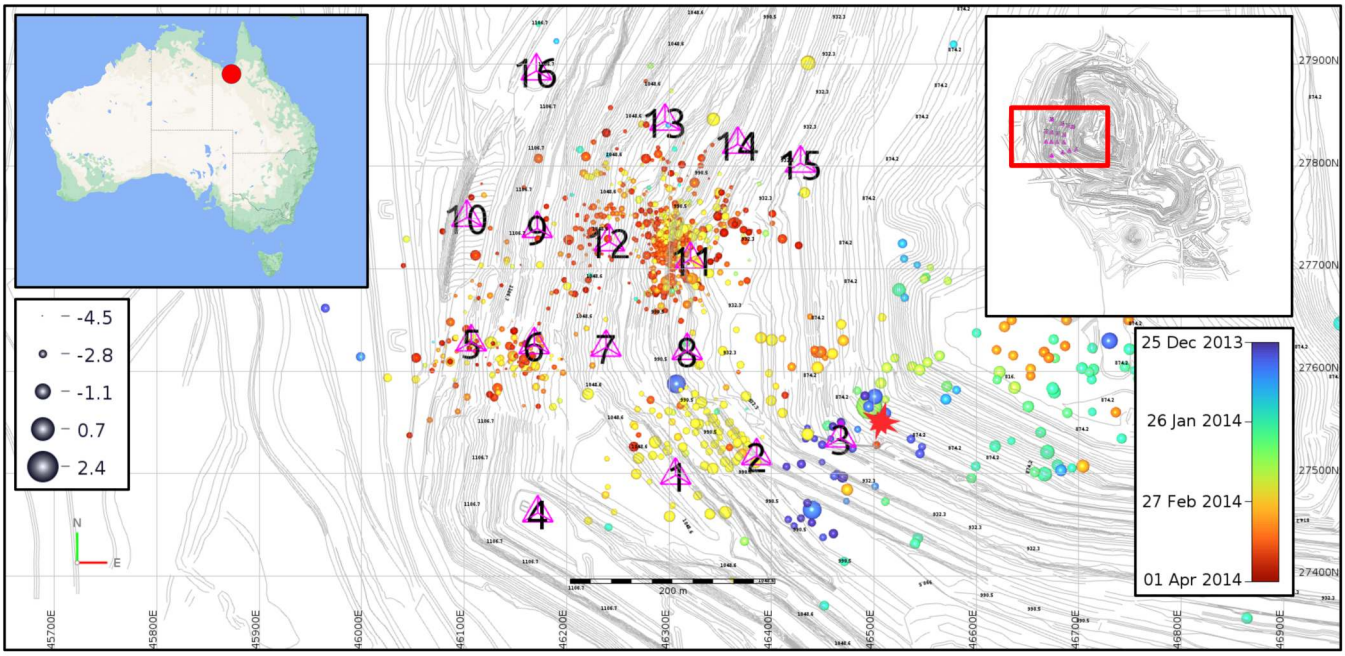

Figure 1 Plan view of the locations of the geophones in the seismic array (magenta triangles) installed below the western slope of the open-pit of Century Mine. The location of the mine within Australia (left inset) and the location of the array within the open-pit are both indicated (red box in right inset). Locations of microseismic events recorded by the geophone array are also shown, coloured according to time and sized according to local magnitude. The location of a blast performed by the mine at the foot of the slope on the 11th of February 2014 at 10:40 local time is indicated by the red explosion symbol.

Ambient seismic noise interferometry has shown tremendous promise in the field of landslide monitoring (Mainsant et al., 2012; Voisin et al., 2016; Le Breton et al., 2021). Notably, Mainsant et al. (2012) used ambient seismic noise correlations to detect precursory velocity changes in a landslide in the Swiss Alps prior to slope failure. Their study highlighted the potential application for the technique in providing early warning to landslide failure. Over the last two decades, seismic noise interferometry has also been applied across a wide range of other settings to monitor time-lapse velocity changes, for example: following large earthquakes (Brenguier et al., 2008a; Hillers et al., 2019); near volcanoes (Snieder and Hagerty, 2004; Brenguier et al., 2008b; Nakata et al., 2016; Donaldson et al., 2017); underneath ice sheets (Mordret et al., 2016); around geothermal reservoirs (Obermann et al., 2015; Hillers et al., 2015); tracking of ground water (Lecocq et al., 2017; Clements and Denolle, 2018); across earthen dams (Planès et al., 2016; Olivier et al., 2017); and in underground mining environments (Olivier et al., 2015; Olivier and Brenguier, 2016; Czarny et al., 2016). The interferometric method relies on the reconstruction of the seismic Green's function between sensors, effectively turning one station into a virtual active source (Curtis et al., 2006). Since these virtual sources contain information about the medium between sensors, this method is able to detect tiny changes in the seismic velocity of the medium.

In this paper we present the first application of seismic interferometry to the monitoring of a slope failure in an open-pit mine. Slope failures in open-pit mines have occurred regularly over the past two decades, with several notable slope failures including: Bingham Canyon mine in the United States of America in 2013 (Hibert et al., 2014); Palabora Mine, South Africa in 2003 (Brummer et al., 2006); Super Pit near Kalgoorie, Australia in 2018 (Darbritz, 2023); and Gamsberg Mine, South Africa, in 2020 (Pretorius et al., 2025). The causes of these various failures have been attributed to a combination of geological structural weaknesses and triggering events such as heavy rainfall or seismic activity.

Future projections for the increased requirement for electrical batteries is expected to generate knock-on demand for minerals that are critical to battery production, such as copper, lithium, and cobalt (IRENA, 2024). The extraction of these minerals will require the establishment of new mines, including open-pit mines, and will expose human populations to the increased risks of associated pit wall slope failures. In this study we demonstrate how seismic noise interferometry is able to play a role in monitoring the slopes of open-pit mines of the future.

2 Data and Methods

The seismic data used in this study was recorded at the Century Mine, an open-cut zinc, lead, and silver mine located in north-east Queensland, Australia (see left inset in Fig. 1). The local geology consists primarily of interbedded sedimentary sequences, dominated by shale and sandstone units, with the western slope

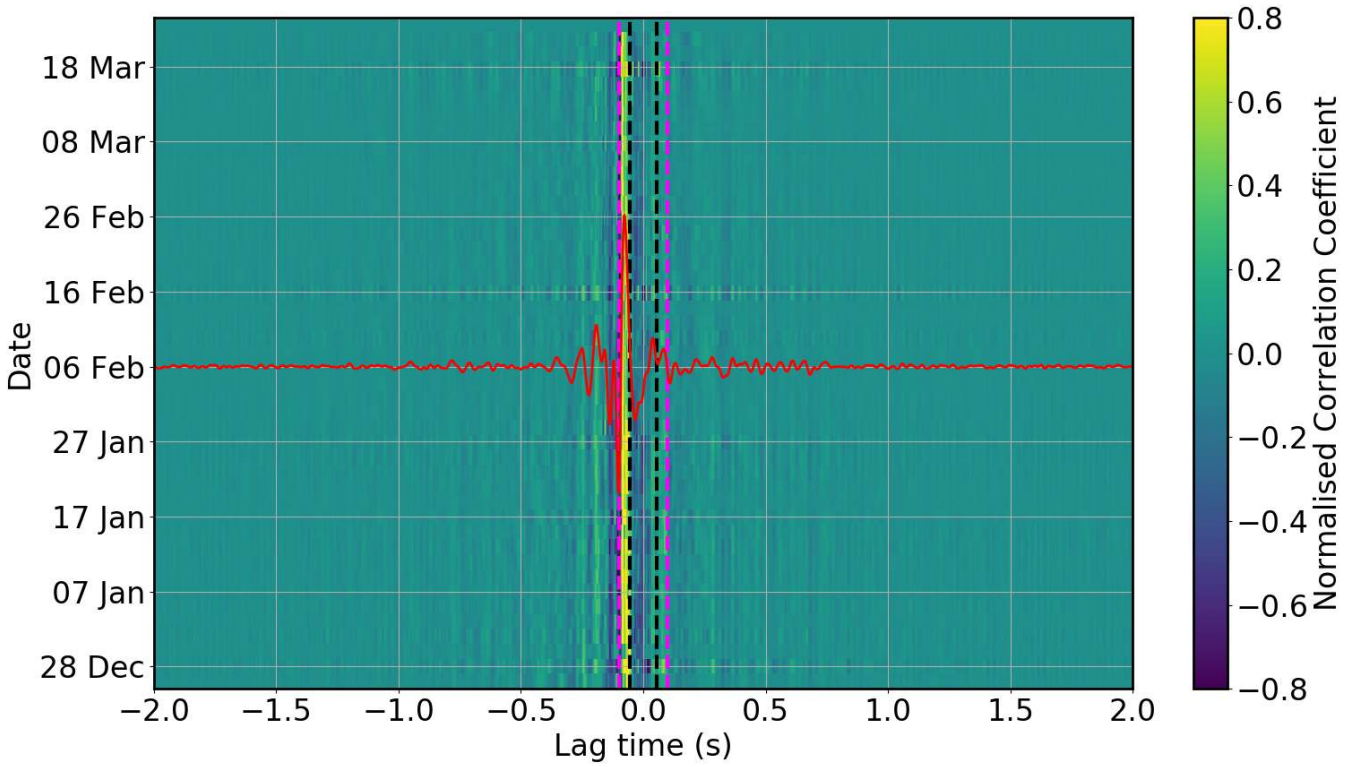

Figure 2 Cross-correlations for sensor component pair 1X and 3Z, shown for lag times in [-2s, 2s] between the 25th of December 2013 and 31st of March 2014 (UTC). The average cross-correlation over this whole period is show as an overlay in red. Dashed vertical lines on both the causal and acausal sides indicate estimates of direct P- and S-wave arrival times (from approximate P-wave velocity of 3.6 km/s and S-wave velocity of 2 km/s).

wall geology consisting of units dominated by black carbonaceous shales (Salvoni and Dight, 2016). While the fresh rock is mechanically competent, the shales have a high clay (montmorillonite) and pyrite content, making them prone to rapid deterioration and slaking upon exposure. The structural setting is complex. A subvertical fault, the Page Creek Fault, intersects the slope, creating a localized zone of highly sheared and fractured rock (Salvoni and Dight, 2016). This combination of lithology and heavy fracturing makes the slope sensitive to external forcing.

In late 2013, an array of 16 geophones (numbered 1 to 16) was installed in four boreholes (Fig. 1), drilled from surface on the perimeter of the open-pit, underneath the western slope face (see right inset in Fig. 1). The original objective of the geophone array was to record and analyse microseismic events to aid in the analysis of slope stability (Meyer, 2015; Salvoni and Dight, 2016; Luo et al., 2018). In addition to the microseismic events, continuous seismic data was also recorded at a sampling rate of 6000 Hz for 2 months prior to a slope failure that occurred on the 23rd February 2014. In this study, we focus on the continuous data recordings. The high-frequencies present in the seismic wavefield in this active mine environment are generated by continuous anthropogenic noise sources, including haul trucks, crushers, and excavation machinery.

To prepare the data for seismic interferometry we processed the continuous waveforms by first decimating the records to a sampling rate of 500 Hz, and demeaning and detrending the resulting time series. One-bit amplitude normalisation was applied, followed by spectral whitening between 5 Hz and 100 Hz (Bensen et al., 2007). The time series were then divided into 10-second windows. To estimate empirical Green's functions, we cross correlated each sensor-component pair within the array and calculated average cross-correlation functions over non-overlapping two-day periods. Although the individual cross-correlations for a particular sensor component pair were consistent, two-day stacking periods were used to ensure stability in time (Hadziioannou et al., 2009). Upon visual inspection of the correlations for all sensor-component pairs, correlations involving the Z-component of sensor 7 appeared to be of poor quality. Subsequent inspection revealed the geophone element to be faulty. Using a homogeneous velocity model calibrated from the analysis of P- and S-wave travel-times from known blasting locations performed at the mine, we were able to identify direct body wave arrivals in many of the cross-correlation functions (for example, see Fig. 2).

To measure temporal variations in seismic velocity throughout the recording period of the seismic array, we applied the Moving Window Cross-Spectrum (MWCS) method (Clarke et al., 2011) to the coda portion of our two-day correlation stacks in the 6 to 30 Hz frequency range. In this frequency range, this coda portion likely consists of surface waves and scattered body waves trapped in the near-surface heterogeneities. The coda portion considered in this study corresponds to lag-times in the correlations between 1.2 times the direct S-wave arrival time and 2s for both the causal and

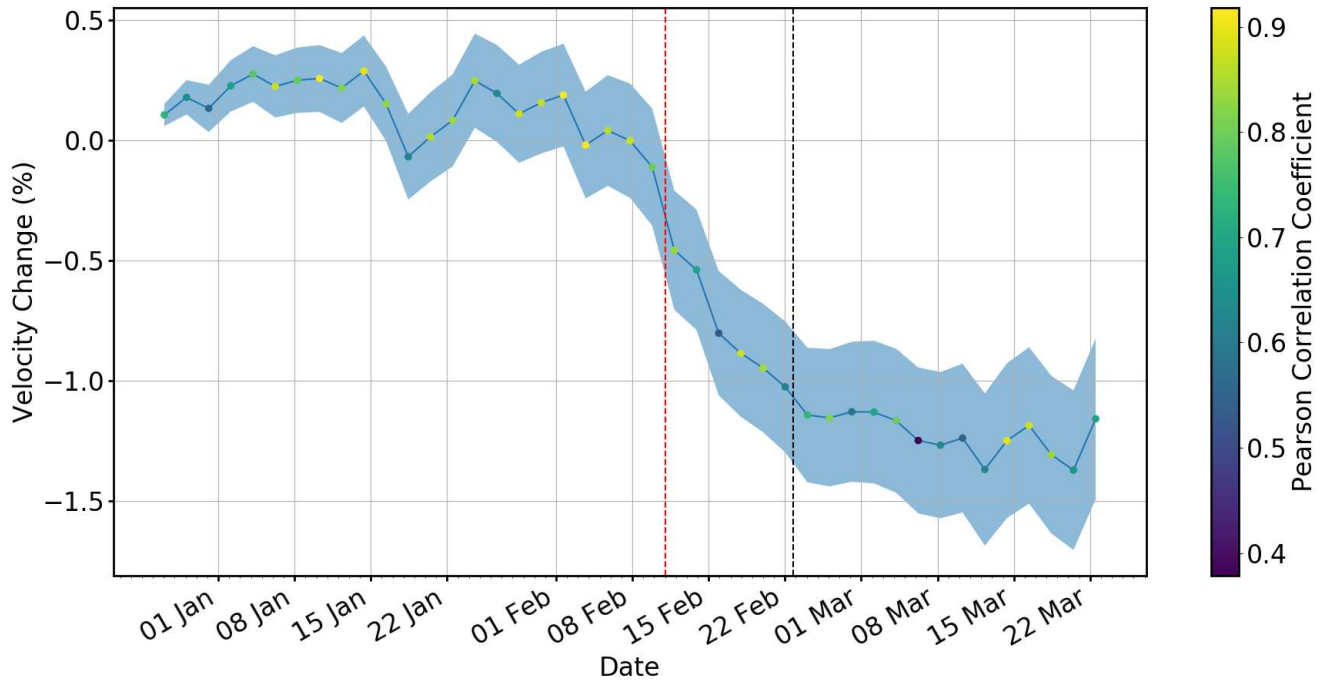

Figure 3 Time-lapse velocity changes calculated using the MWCS method from correlations of the same sensor component pair shown in Fig. 2 (1X and 3Z) between the 25th of December 2013 and 31st of March 2014 (UTC). Measurements are coloured according to the correlation coefficient between current and reference stacks. Uncertainties in these measurements are indicated by the shaded region. The black dashed line indicates when the slope first began to fail. Velocity change observations are plotted at the centre time of the 2-day correlation window used to measure the change.

acausal sides of the correlation. This window seeks to avoid the direct arrivals while capturing the multiply scattered energy most sensitive to medium changes.

The MWCS approach measures a phase shift (δt) within a defined lag-time window. We utilised a lag-time window of length 0.17 s, which contains at least one full period at the lowest frequency of interest in the correlation functions. We overlap our measurement windows by 0.02s (90%) to increase the number of measurements and reduce the uncertainty in phase shift measurements. Assuming a homogeneous velocity change in the medium, a weighted linear regression of these phase shifts can be used to measure a change in velocity (using $\delta v/v = -\delta t/t$) and the associated uncertainties. The weighting of the regression is the coherency of the waveforms in each lag-time window (Clarke et al., 2011). We calculate these relative velocity changes between consecutive 2-day stacks (a moving reference) to maintain high coherency. These incremental changes are then accumulated to produce the time-lapse velocity variation series shown in the results. Velocity changes (given as a percentage) in Fig. 3 are those calculated from correlations of the same sensor component pair shown in Fig. 2 (1X and 3Z) between the 25th of December 2013 and 31st of March 2014.

3 Results and Interpretation

Time-lapse velocity changes (and associated uncertainties) were measured using the MWCS method for each of the 476 sensor-component pairs in the array as outlined in Section 2. Fig. 4 shows the average of these changes across all sensor-component pairs. The initialisation of slope failure on the 23rd of February 2014 is indicated by the dashed black line. Also shown in Fig. 4 is the daily rainfall (in mm) recorded at the nearby Australian Bureau of Meteorology Station also located at the mine (YCNY). Line-of-sight slope displacement measurements (in mm) from ground-based radar and the cumulative number (and associated local magnitudes) of recorded microseismic events are also included in Fig. 4. Positive displacements represent movement out of the slope, towards the radar sensor.

The initiation of slope failure closely coincides with a two day period of heavy rainfall (around 50mm per day). It is also clear from Fig. 4 that the rate of recorded seismicity began to increase only as the open-pit slope started to fail. Similarly, while line-of-sight slope displacement is detected in some parts of the slope prior to the failure (particularly following the heaviest rainfall day of 115 mm on the 16th of February 2014), significant displacements are only measured after the slope began to fail. In contrast, our measured seismic velocity changes begin to decrease approximately two weeks prior to the slope failure (between two-day cross-correlation stacks centered on the 9th and 11th of February 2014). We also observe a slight increase in velocity prior to the initial velocity decrease. This trend likely corresponds to the drying and stiffening of the shallow subsurface material during the relatively dry period preceding this.

The seismic velocity changes presented in Fig. 4 indicate a precursory decrease in seismic velocity prior slope failure. A similar observation was made prior to

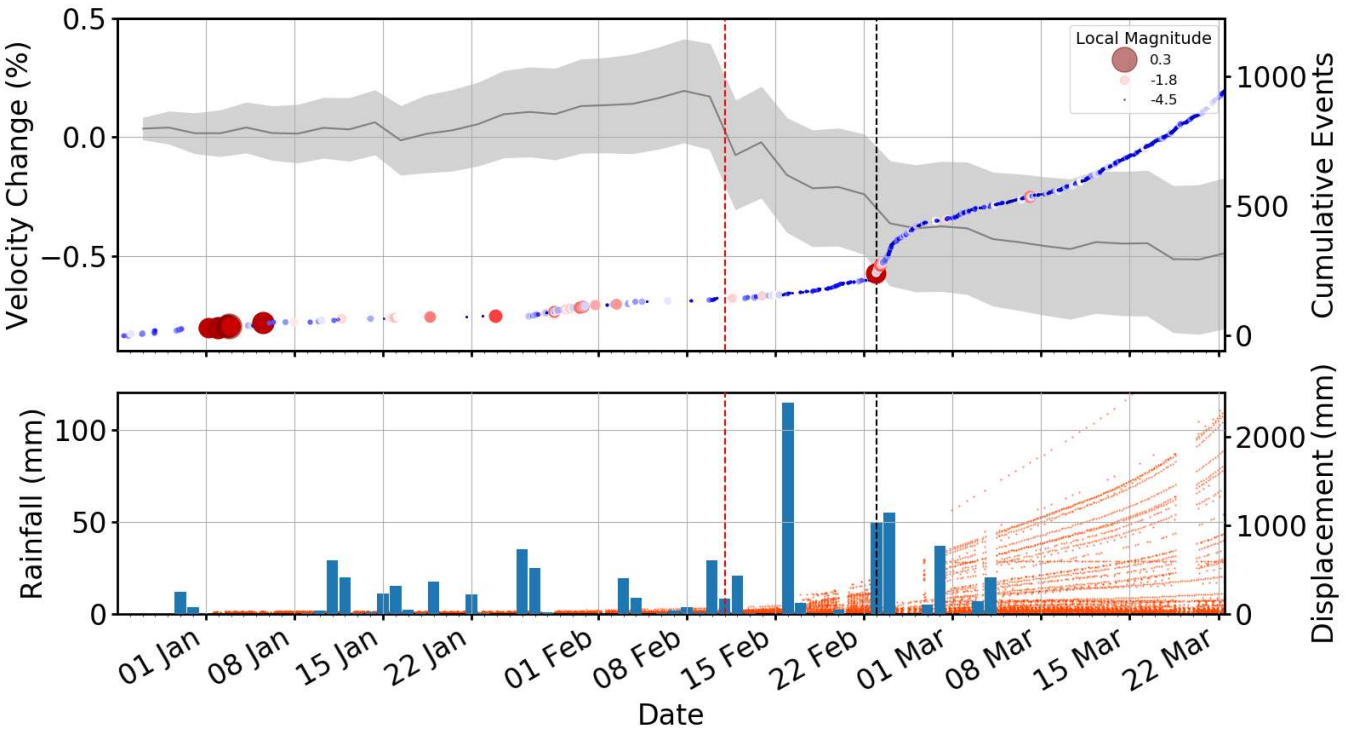

Figure 4 Time-lapse velocity changes averaged across all sensor component pairs calculated using the MWCS method between the 25th of December 2013 and 31st of March 2014 (grey) and shaded region indicating the cumulative average uncertainty in the measurements across all sensor component pairs (top). Velocity change observations are plotted at the centre time of the 2-day correlation window used to measure the change. The cumulative number of recorded seismic events during this same period is also shown in the top Fig. (coloured and sized according to local magnitude). Daily rainfall (blue) recorded at the nearby Australian Bureau of Meteorology Station at the mine: code YCNY (bottom). Time-lapse line-of-sight displacement measurements (orange points) from ground-based radar (bottom). Red and black dashed lines indicate the approximate times of the blast and when the slope first began to fail respectively.

the landslide failure case of Mainsant et al. (2012) in the Swiss Alps, but uniquely, the seismic velocity decrease that we detect in the present study was distinctly sharp for all sensor-component pairs.

On further investigation, we discovered that the onset of the seismic velocity decrease coincided with the largest ground motion recorded at the array during recording (41 mm/s recorded by sensor 3). This ground motion originated from a blast performed by the mine at the foot of the slope on the 11th of February 2014 at 10:40 local time. The blast (with a dominant frequency between 10 and 15 Hz) was located from phase arrival picking (indicated by the explosion symbol in Fig. 1).

Co-seismic velocity decreases following a large ground motions are a common phenomena, and are generally attributed to "co-seismic damage in the shallow layers and to deep co-seismic stress change and post-seismic stress relaxation" (Brenguier et al., 2008a). Though we believe the co-seismic velocity decrease detected at Century Mine following the blast can similarly be related to co-seismic damage of the shallow subsurface below the slope face, we note that in this case seismic velocities continue to decrease for a further 12 days until the slope begins to fail. The sharpness of the observed velocity drop, compared to the gradual changes from creep observed in natural landslides (e.g., Mainsant et al. 2012), reflects the impulsive nature of the blast source causing immediate co-seismic damage. Furthermore, the 6–30 Hz frequency band is highly sensitive to changes in the shallow, weathered layer of the slope, which would have been most susceptible to the shaking from this blast. The continued decrease in seismic velocity could be attributed to the heavy rainfall a few days after the blast (115 mm on the 16th of February 2014), causing water to to seep into existing fault structures, weakening or softening them, or even into newly formed cracks (following co-seismic damage from the blast) of the shallow subsurface below the slope face.

While the average seismic velocity change across all sensor-component pairs was approximately -0.5% for the period between the blast and the onset of failure (Fig. 4), the magnitude of this change varied spatially. Several sensor pairs observed decreases significantly larger than the average; for example, pair 1X-3Z observed a change of approximately -1.0% (Fig. 3).

We analyzed the statistics of these variations to check for directional dependencies. The velocity changes observed across different cross-components of common sensor pairs were consistent (average standard deviation of 0.16%), and no specific component combinations (e.g., X-X, Y-Z) or azimuthal directions of the sensor pairs showed significantly different velocity changes. This lack of directionality suggests that the coda waves used were sufficiently scattered to sample the medium without strong bias from the source-receiver orientation.

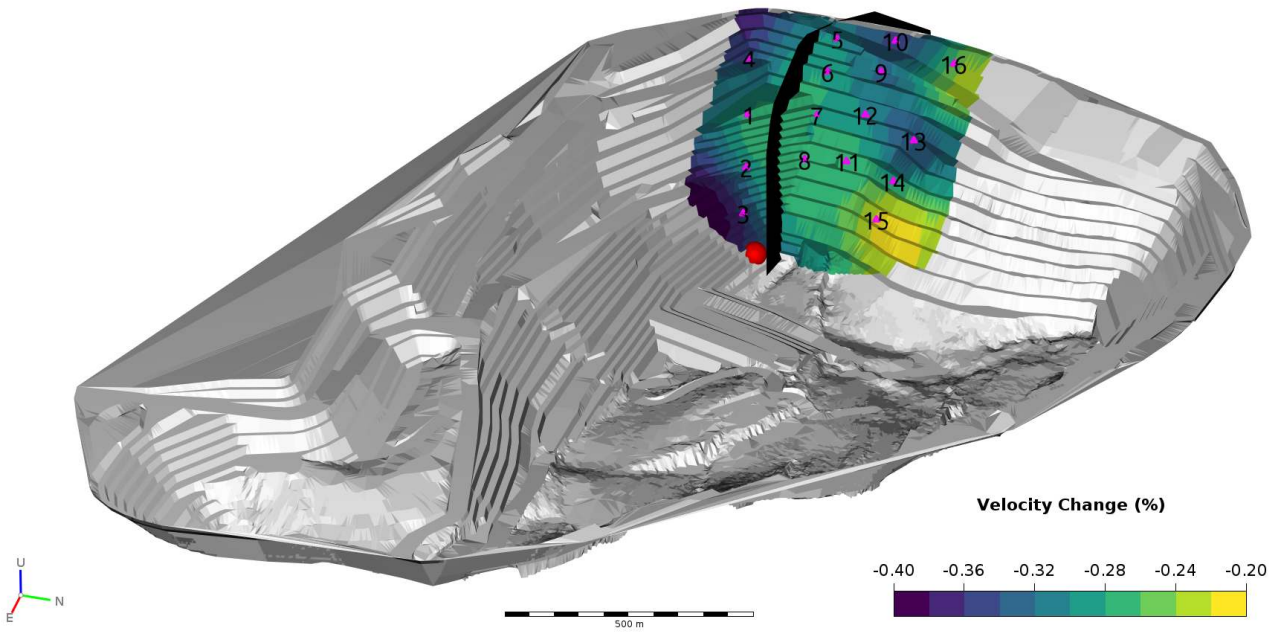

Figure 5 Spatial interpolation of time-lapse velocity changes on the slope surface, averaged for the period between the blast event and the onset of slope failure. The red sphere marks the location of the blast source, and the black plane represents the approximate trace of the Page Creek Fault.

3.1 Regionalisation

In order to gain an understanding of how the temporal variations in seismic velocity are distributed in 3D space, we follow the procedure of Brenguier et al. (2008b). Though a more rigorous approach to examining spatial variations in velocity changes measured using coda-wave interferometry could be undertaken by calculating spatial sensitivity kernels for each sensor pair (Obermann et al., 2013; Kanu and Snieder, 2015; Obermann et al., 2016, 2019), the density and regular distribution of sensors throughout the array at Century Mine allowed the simplified approach to provide good insight into the spatial variations in velocity changes measured.

Velocity changes from each of the 476 sensor component pairs are averaged for each sensor according to the pairs with which it was constituent. As sensitivity kernels associated with coda-wave interferometry are peaked around sensor locations, the average velocity changes for each sensor are interpolated onto a grid on the slope surface relative to its proximity to each sensor location (inverse square of distance). Spatial variations of velocity changes in the time period following the blast and leading up to when the slope first began to fail are shown in Fig. 5 (time period between red and black dashed lines in Fig. 4). The southern part of the slope region shows large decreases in seismic velocity, which coincides with the Page Creek fault and the part of the slope that first began to fail (Salvoni and Dight, 2016). The largest decreases in seismic velocity were detected near the bottom of the pit, in close proximity to the location of the blast. This supports the suggestion that the seismic velocity decrease detected in this region is related to co-seismic damage of the shallow subsurface below the slope face from the blast performed nearby.

4 Conclusions

We have presented observations of time-lapse velocity variations from a dense array of geophones installed beneath the slope of an open-pit mine during an episode of slope failure. Our time-lapse seismic velocity observations show a precursory decrease approximately 12 days prior to the slope initiating failure. This velocity decrease coincided with a blast performed by the mine near the foot of the slope, indicating possible co-seismic damage to the slope as the initial source of these velocity changes. Most interestingly, these initial velocity changes were detected in the absence of an increase in the rate of recorded microseismic activity or significant surface displacement in the slope itself. Approximately a week before the slope failure, heavy rainfall appears to drive further decreases in seismic velocity, possibly due to water seeping into existing fault structures, weakening or softening them, or even into newly formed cracks (following co-seismic damage from the blast).

In this study we have demonstrated the potential for seismic noise interferometry in detecting precursory velocity variations in the subsurface that may indicate an impending slope failure in open-pit mines. With many mines likely to be built over the next decade to meet increased demands for minerals, seismic interferometry might play a key role in preventing such failures. This would potentially save lives and significantly reduce the economic impact to the mine.

Acknowledgements

We thank the Institute of Mine Seismology for their technical and financial support that made this research possible. We are also thankful for support of the original project by MMG Century mine (in particular the original staff on site that facilitated monitoring logistics, namely, Erin Sweeney, Kyle Abbott and Claudio Coimbra) and for permission to use and publish the data. We are also grateful for research discussions with Dr. George Taylor, Robert Hill, Dr. Gerrit Olivier and Richard Gillies. We thank the editor and two anonymous reviewers for their constructive comments and suggestions, which significantly improved the clarity and interpretation of this manuscript.

Data and code availability

The data used in this study (cross-correlations, velocity change measurements, seismic event information, historical weather and surface deformation data) are archived on Zenodo and can be found at doi: 10.5281/zenodo.14969229 (T. de Wit and R. Snieder, 2025). The MWCS function from version 1.6 of the MSNoise package (Lecocq et al., 2014) was used to make the velocity change measurements presented in this study. The Matplotlib library version 3.1.1 in python was used to generate the figures.

Competing interests

The authors have no competing interests.

References

Bensen, G. D., Ritzwoller, M. H., Barmin, M. P., Levshin, A. L., Lin, F., Moschetti, M. P., Shapiro, N. M., and Yang, Y. Processing seismic ambient noise data to obtain reliable broad-band surface wave dispersion measurements. *Geophysical Journal International*, 169(3):1239–1260, 2007. doi: 10.1111/j.1365-246X.2007.03374.x.

Brenguier, F., Campillo, M., Hadziioannou, C., Shapiro, N. M., Nadeau, R. M., and Larose, E. Postseismic relaxation along the San Andreas fault at Parkfield from continuous seismological observations. *Science*, 321(5895):1478–1481, 2008a. doi: 10.1126/science.1160943.

Brenguier, F., Shapiro, N. M., Campillo, M., Ferrazzini, V., Duputel, Z., Coutant, O., and Nercessian, A. Towards forecasting volcanic eruptions using seismic noise. *Nature Geoscience*, 1(2):126–130, 2008b. doi: 10.1038/ngeo104.

Brummer, R. K., Li, H., and Moss, A. THE TRANSITION FROM OPEN PIT TO UNDERGROUND MINING: AN UNUSUAL SLOPE FAILURE MECHANISM AT PALABORA. In *International Symposium on Stability of Rock Slopes in Open Pit Mining and Civil Engineering*, pages 411–420, 2006.

Carlà, T., Tofani, V., Lombardi, L., Raspini, F., Bianchini, S., Bertolo, D., Thuegaz, P., and Casagli, N. Combination of GNSS, satellite InSAR, and GBInSAR remote sensing monitoring to improve the understanding of a large landslide in high alpine environment. *Geomorphology*, 335:62–75, 2019. doi: 10.1016/j.geomorph.2019.03.014.

Clarke, D., Zaccarelli, L., Shapiro, N. M., and Brenguier, F. Assessment of resolution and accuracy of the Moving Window Cross Spectral technique for monitoring crustal temporal variations using ambient seismic noise. *Geophysical Journal International*, 186(2):867–882, 2011. doi: 10.1111/j.1365-246X.2011.05074.x.

Clements, T. and Denolle, M. A. Tracking Groundwater Levels Using the Ambient Seismic Field. *Geophysical Research Letters*, 45(13):6459–6465, 2018. doi: 10.1029/2018GL077706.

Curtis, A., Gerstoft, P., Sato, H., Snieder, R., and Wapenaar, K. Seismic interferometry - Turning noise into signal. *The Leading Edge*, 25(9):1082–1092, 2006. doi: 10.1190/1.2349814.

Czarny, R., Marcak, H., Nakata, N., Pilecki, Z., and Isakow, Z. Monitoring Velocity Changes Caused By Underground Coal Mining Using Seismic Noise. *Pure and Applied Geophysics*, 173(6):1907–1916, 2016. doi: 10.1007/s00024-015-1234-3.

Darbritz, J. Management of the Kalgoorlie Consolidated Gold Mines East Wall Slip. In *SSIM 2023: Third International Slope Stability in Mining Conference*, number August 2022, pages 695–704, 2023. doi: 10.36487/ACG_repo/2335_47.

Donaldson, C., Caudron, C., Green, R. G., Thelen, W. A., and White, R. S. Relative seismic velocity variations correlate with deformation at Kīlauea volcano. *Science Advances*, 3(6):e1700219, 2017. doi: 10.1126/sciadv.1700219.

Froude, M. J. and Petley, D. N. Global fatal landslide occurrence from 2004 to 2016. *Natural Hazards and Earth System Sciences*, 18(8):2161–2181, 2018. doi: 10.5194/nhess-18-2161-2018.

Gariano, S. L. and Guzzetti, F. Landslides in a changing climate. *Earth-Science Reviews*, 162:227–252, 2016. doi: 10.1016/j.earscirev.2016.08.011.

Hadziioannou, C., Larose, E., Coutant, O., Roux, P., and Campillo, M. Stability of Monitoring Weak Changes in Multiply Scattering Media with Ambient Noise Correlation: Laboratory Experiments. *Journal of the Acoustical Society of America*, 125:1–10, 2009. doi: 10.1121/1.3125345.

Hibert, C., Ekström, G., and Stark, C. P. Dynamics of the Bingham Canyon Mine landslides from seismic signal analysis. *Geophysical Research Letters*, (May):4535–4541, 2014. doi: 10.1002/2014GL060592.Joint.

Hillers, G., Husen, S., Obermann, A., Planès, T., Larose, E., and Campillo, M. Noise-based monitoring and imaging of aseismic transient deformation induced by the 2006 Basel reservoir stimulation. *Geophysics*, 80(4):KS51–KS68, 2015. doi: 10.1190/geo2014-0455.1.

Hillers, G., Campillo, M., Brenguier, F., Moreau, L., Agnew, D. C., and Ben-Zion, Y. Seismic Velocity Change Patterns Along the San Jacinto Fault Zone Following the 2010 M7.2 El Mayor-Cucapah and M5.4 Collins Valley Earthquakes. *Journal of Geophysical Research: Solid Earth*, 124(7):7171–7192, 2019. doi: 10.1029/2018JB017143.

IRENA. Critical materials: Batteries for electric vehicles. Technical report, International Renewable Energy Agency, Abu Dhabi, 2024. https://www.irena.org/Publications/2024/Sep/Critical-materials-Batteries-for-electric-vehicles.

Kanu, C. and Snieder, R. Time-lapse imaging of a localized weak change with multiply scattered waves using numerical-based sensitivity kernel. *Journal of Geophysical Research: Solid Earth*, 120(8):5595–5605, 2015. doi: 10.1002/2015JB011871.

Le Breton, M., Bontemps, N., Guillemot, A., Baillet, L., and Larose, É. Landslide monitoring using seismic ambient noise correlation: challenges and applications. *Earth-Science Reviews*, 216(December 2020):103518, 2021. doi: 10.1016/j.earscirev.2021.103518.

Lecocq, T., Caudron, C., and Brenguier, F. MSNoise, a Python Package for Monitoring Seismic Velocity Changes Using Ambient Seismic Noise. *Seismological Research Letters*, 85(3):715–726,

05 2014. doi: 10.1785/0220130073.

Lecocq, T., Longuevergne, L., Pedersen, H. A., Brenguier, F., and Stammler, K. Monitoring ground water storage at mesoscale using seismic noise: 30 years of continuous observation and thermo-elastic and hydrological modeling. *Scientific Reports*, 7(1):1–16, 2017. doi: 10.1038/s41598-017-14468-9.

Lissak, C., Bartsch, A., De Michele, M., Gomez, C., Maquaire, O., Raucoules, D., and Roulland, T. Remote Sensing for Assessing Landslides and Associated Hazards. *Surveys in Geophysics*, 41 (6):1391–1435, 2020. doi: 10.1007/s10712-020-09609-1.

Luo, X., Salvoni, M., Dight, P., and Duan, J. Microseismic events for slope stability analysis — a case study at an open pit mine. *Journal of the Southern African Institute of Mining and Metallurgy*, 118 (3):205–210, 2018. doi: 10.17159/2411-9717/2018/v118n3a2.

Mainsant, G., Larose, E., Brnnimann, C., Jongmans, D., Michoud, C., and Jaboyedoff, M. Ambient seismic noise monitoring of a clay landslide: Toward failure prediction. *Journal of Geophysical Research: Earth Surface*, 117(1):F01030, 2012. doi: 10.1029/2011JF002159.

Meyer, S. Slope deformation mechanics from microseismic monitoring. In *International Symposium on Rock Slope Stability in Open Pit and Civil Engineering*, pages 181–194. The Southern African Institute of Mining and Metallurgy, Cape Town, 2015.

Mordret, A., Mikesell, T. D., Harig, C., Lipovsky, B. P., and Prieto, G. A. Monitoring southwest Greenland's ice sheet melt with ambient seismic noise. *Science Advances*, 2(5):e1501538, 2016. doi: 10.1126/sciadv.1501538.

Nakata, N., Boué, P., Brenguier, F., Roux, P., Ferrazzini, V., and Campillo, M. Body and surface wave reconstruction from seismic noise correlations between arrays at Piton de la Fournaise volcano. *Geophysical Research Letters*, 43(3):1047–1054, 2016. doi: 10.1002/2015GL066997.

Obermann, A., Planès, T., Larose, E., Sens-Schönfelder, C., and Campillo, M. Depth sensitivity of seismic coda waves to velocity perturbations in an elastic heterogeneous medium. *Geophysical Journal International*, 194(1):372–382, 2013. doi: 10.1093/gji/ggt043.

Obermann, A., Kraft, T., Larose, E., and Wiemer, S. Potential of ambient seismic noise techniques tomonitor the St. Gallen geothermal site (Switzerland). *Journal of Geophysical Research: Solid Earth*, 120(6):4301–4316, 2015. doi: 10.1002/2014JB011817.

Obermann, A., Planés, T., Hadziioannou, C., and Campillo, M. Lapse-time-dependent coda-wave depth sensitivity to local velocity perturbations in 3-D heterogeneous elastic media. *Geophysical Journal International*, 207(1):59–66, 2016. doi: 10.1093/gji/ggw264.

Obermann, A., Planès, T., Larose, E., and Campillo, M. 4-D Imaging of Subsurface Changes with Coda Waves: Numerical Studies of 3-D Combined Sensitivity Kernels and Applications to the Mw 7.9, 2008 Wenchuan Earthquake. *Pure and Applied Geophysics*, 176(3):1243–1254, 2019. doi: 10.1007/s00024-018-2014-7.

Olivier, G. and Brenguier, F. Interpreting seismic velocity changes observed with ambient seismic noise correlations. *Interpretation*, 4(3):SJ77–SJ85, 2016. doi: 10.1190/INT-2015-0203.1.

Olivier, G., Brenguier, F., Campillo, M., Lynch, R., and Roux, P. Body-wave reconstruction from ambient seismic noise correlations in an underground mine. *Geophysics*, 80(3):KS11–KS25, 2015. doi: 10.1190/geo2014-0299.1.

Olivier, G., Brenguier, F., de Wit, T., and Lynch, R. Monitoring the stability of tailings dam walls with ambient seismic noise. *The Leading Edge*, 36(4):350a1–350a6, 2017. doi: 10.1190/tle36040350a1.1.

Petley, D. Global patterns of loss of life from landslides. *Geology*, 40(10):927–930, 10 2012. doi: 10.1130/G33217.1.

Planès, T., Mooney, M. A., Rittgers, J. B. R., Parekh, M. L., Behm, M., and Snieder, R. Time-lapse monitoring of internal erosion in earthen dams and levees using ambient seismic noise. *Géotechnique*, 66(4):301–312, 2016. doi: 10.1680/jgeot.14.P.268.

Pretorius, M., Bas, P., Pretorius, J., Gkikas, I., and Narshai, P. Informing an operational slope stability feedback loop : integrating InSAR monitoring and 3D modelling at Gamsberg Mine. In *SSIM 2025: Fourth International Slope Stability in Mining Conference*, pages 1–15, 2025. doi: 10.36487/ACG_repo/2535_52.

Salvoni, M. and Dight, P. M. Rock damage assessment in a large unstable slope from microseismic monitoring - MMG Century mine (Queensland, Australia) case study. *Engineering Geology*, 210: 45–56, 2016. doi: 10.1016/j.enggeo.2016.06.002.

Sim, K. B., Lee, M. L., and Wong, S. Y. A review of landslide acceptable risk and tolerable risk. *Geoenvironmental Disasters*, 9(1):3, 2022. doi: 10.1186/s40677-022-00205-6.

Snieder, R. and Hagerty, M. Monitoring change in volcanic interiors using coda wave interferometry: Application to Arenal Volcano, Costa Rica. *Geophysical Research Letters*, 31(9):L09608, 2004.

T. de Wit and R. Snieder. Did they blow it? *Dataset on Zenodo*, 2025. doi: 10.5281/zenodo.14969229.

Voisin, C., Garambois, S., Massey, C., and Brossier, R. Seismic noise monitoring of the water table in a deep-seated, slow-moving landslide. *Interpretation*, 4(3):SJ67–SJ76, 2016. doi: 10.1190/INT-2016-0010.1.

Wieczorek, G. F. *Landslides: investigation and mitigation*. National Academy Press, Washington, D.C., 1996. http://onlinepubs.trb.org/Onlinepubs/sr/sr247/sr247-004.pdf.